Weak phases from B decays to kaons and charged pions

Amol S. Dighe
Enrico Fermi Institute and Department of Physics, University of Chicago, Chicago, Illinois 60637

Michael Gronau
Department of Physics, Technion—Israel Institute of Technology, Haifa 32000, Israel

Jonathan L. Rosner
Div. TH, CERN, 1211 CH Geneva 23, Switzerland
*and Enrico Fermi Institute and Department of Physics, University of Chicago, Chicago, Illinois 60637**

(Received 8 April 1996)

Phases of elements of the Cabibbo-Kobayashi-Maskawa (CKM) matrix can be obtained using decays of B mesons to $\pi^+\pi^-$, $\pi^\pm K^\mp$, and π^+K^0 or $\pi^-\bar{K}^0$. For B^0 or $\bar{B}^0 \to \pi^+\pi^-$, one identifies the flavor of the neutral B meson at time of production and studies the time dependence of the decay rate. The other processes are self-tagging and only their rates need to be measured. By assuming flavor SU(3) symmetry and first-order SU(3) breaking, one can separately determine the phases $\gamma \equiv \mathrm{Arg}\, V_{ub}^*$ and $\alpha = \pi - \beta - \gamma$, where $\beta \equiv \mathrm{Arg}\, V_{td}^*$. Special cases include the vanishing of strong interaction phase differences between amplitudes, the possibility of recovering partial information when $\pi^+\pi^-$ and $\pi^\pm K^\mp$ decays cannot be distinguished from one another, and the use of a correlation between γ and α in the region of allowed parameters. [S0556-2821(96)01617-7]

PACS number(s): 12.15.Hh, 11.30.Er, 13.25.Hw, 14.40.Nd

I. INTRODUCTION

The decays of B mesons [1] offer the prospect of confirming or refuting the current explanation of CP violation in the neutral kaon system [2], based on phases in the Cabibbo-Kobayashi-Maskawa (CKM) matrix [3]. For example, unequal time-integrated rates for the $\pi^+\pi^-$ decays of states which are initially B^0 and and $\bar{B}^0$ would signify CP violation, providing approximate information on the angle α of the triangle describing the unitarity of the CKM matrix.

The presence of gluonic [4] and electroweak [5] penguin contributions in additional to the dominant (''tree'') processes requires that one separate out several terms. An isospin analysis [6], involving the study of the time dependence of the $\pi^+\pi^-$ mode and rates for the $\pi^\pm\pi^0$ and $\pi^0\pi^0$ modes of B mesons, permits one to isolate the amplitudes contributing to final states with isospin 0 and 2 and thereby to determine α rather well [6,7]. However, for certain types of detectors, the observation of neutral pions may pose a challenge, and model calculations [8] predict a branching ratio for $B^0 \to \pi^0\pi^0$ of order 10^{-6} or less.

A few alternative ways to sort out the effects of several amplitudes in $B^0 \to \pi^+\pi^-$ were suggested recently. DeJongh and Sphicas [9] studied the dependence of the asymmetry in $B^0(t) \to \pi^+\pi^-$ on the magnitude and relative phase of the contributing terms. Using flavor SU(3) symmetry, Silva and Wolfenstein [10] estimated the penguin contribution by comparing the tree-dominated decay rate of $B^0 \to \pi^+\pi^-$ with that of $B^0 \to \pi^- K^+$ which has a large penguin term. Buras and Fleischer [11] proposed relating the penguin term in $B^0 \to \pi^+\pi^-$ via SU(3) to the time-dependent asymmetry of $B^0(t) \to K^0\bar{K}^0$, where the penguin amplitude dominates. Kramer, Palmer, and Wu [12] note that the ratio of penguin to tree matrix elements is less model dependent than either quantity alone, and thereby obtain a relation for α. Aleksan *et al.* [13] use model-dependent assumptions to learn the magnitude of the penguin effect on the measurement of α by relating the three $\Delta S = 0$ decay modes $\pi\pi$, $\pi\rho$, and $\rho\rho$ to the corresponding $\Delta S = 1$ modes πK, πK^*, ρK, and ρK^*.

In this paper we examine in more detail a method proposed in [14] to determine phases of CKM matrix elements by detecting only kaons and charged pions in B meson decays. In the decays $B^0 \to \pi^+\pi^-$ and $\bar{B}^0$ to $\pi^+\pi^-$, one identifies the flavor of the neutral B meson at time of production and studies the time dependence of the decay rate. One obtains the necessary information on additional amplitudes from the rates $\Gamma(B^0 \to \pi^- K^+)$, $\Gamma(\bar{B}^0 \to \pi^+ K^-)$, and $\Gamma(B^+ \to \pi^+ K^0)$ or $\Gamma(B^- \to \pi^+ \bar{K}^0)$ using flavor SU(3) symmetry [10,15–18] and first-order SU(3) breaking [19]. In the most general case we obtain information not only on α, but also on $\gamma = \mathrm{Arg}(V_{ub}^*)$ and on strong phase-shift differences. Other ways to measure γ, based on charged B decays, were proposed in [20].

In Sec. II we describe the processes to be measured and the amplitudes on which they depend. We then study the precision to which various quantities can be determined. It is possible that the strong-interaction phase-shift difference δ between amplitudes is below detectable levels, in which case simplified analyses become necessary. Several of these cases are discussed in Sec. III. The most general error analysis (for $\delta \neq 0$) is performed in Sec. IV, while Sec. V concludes. The Appendix is devoted to an aspect of Monte Carlo programs.

*Permanent address.

II. PROCESSES AND AMPLITUDES

A. Expressions for amplitudes and quantities quadratic in them

We review the method proposed in [14], which may be consulted for details. Our method employs flavor SU(3) symmetry [15–17], and neglects ''annihilation'' amplitudes in which the spectator quark (the light quark accompanying the b in the initial meson) enters into the decay Hamiltonian [18]. These amplitudes in B decays are expected to be suppressed by f_B/m_B, where $f_B \simeq 180$ MeV. We include first-order SU(3)-breaking terms [19], expected to be at most tens of percent, but neglect corrections expected to arise at a level of a few percent.

In the SU(3) limit and neglecting annihilation terms, all B decay amplitudes into $\pi\pi$, πK, and KK states can be decomposed in terms of three independent amplitudes [7,18]: a ''tree'' term $t(t')$, a ''color-suppressed'' term $c(c')$, and a ''penguin'' term $p(p')$. These amplitudes contain both the leading-order and electroweak penguin [5] contributions:

$$\begin{aligned} t &\equiv T + (c_u - c_d) P^C_{\rm EW}, \\ c &\equiv C + (c_u - c_d) P_{\rm EW}, \\ p &\equiv P + c_d P^C_{\rm EW}. \end{aligned} \tag{1}$$

Here the capital letters denote the leading-order contributions defined in [18], and $P_{\rm EW}$ and $P^C_{\rm EW}$ are color-favored and color-suppressed electroweak penguin amplitudes defined in [7]. The values $c_u = 2/3$ and $c_d = -1/3$ are those which would follow if the electroweak penguin coupled to quarks in a manner proportional to their charges. (Small corrections, which we shall ignore and which do not affect our analysis, arise from axial-vector Z couplings and from WW box diagrams.) The $\Delta S = 0$ amplitudes are denoted by unprimed quantities and the $\Delta S = 1$ processes by primed quantities.

The amplitudes of the two processes $B^0 \to \pi^+\pi^-$ and $B^0 \to \pi^- K^+$ are expressed as

$$\begin{aligned} A_{\pi\pi} &\equiv A(B^0 \to \pi^+\pi^-) = -t - p = -T - P - \frac{2}{3} P^C_{\rm EW}, \\ A_{\pi K} &\equiv A(B^0 \to \pi^- K^+) = -t' - p' = -T' - P' - \frac{2}{3} P'^C_{\rm EW}, \end{aligned} \tag{2}$$

while that for $B^+ \to \pi^+ K^0$ will be approximated by

$$A_+ \equiv A(B^+ \to \pi^+ K^0) = p' = P' - \frac{1}{3} P'^C_{\rm EW} \approx P' + \frac{2}{3} P'^C_{\rm EW}, \tag{3}$$

neglecting a color-suppressed electroweak penguin effect of order $|P'^C_{\rm EW}/P'| = O((1/5)^2)$ [7]. With this approximation, A_+ contains the same combination of electroweak and gluonic penguins as in the expression for $A_{\pi K}$.

The terms on the right-hand sides of Eqs. (2) and (3) carry well-defined weak phases. The weak phase of T is $\mathrm{Arg}(V_{ud}V^*_{ub}) = \gamma$, and that of $P + (2/3)P^C_{\rm EW}$ is approximately $\mathrm{Arg}(V_{td}V^*_{tb}) = -\beta$, where we neglect corrections due to quarks other than the top quark. The effects of the u and c quarks become appreciable [21] when V_{td} obtains its currently allowed smallest values. This corresponds to a small deviation of the CP asymmetry in $B^0(t) \to \pi^+\pi^-$ from $\sin(2\alpha)\sin(\Delta m t)$ (where Δm is the neutral B mass difference). For large values of V_{td}, where the deviation due to the penguin amplitude becomes significant [22], the u and c contributions become very small. T' also carries the phase γ, while the weak phase of $P' + (2/3)P'^C_{\rm EW}$ is $(V_{ts}V^*_{tb}) = \pi$.

In what follows we shall denote $\mathcal{T} \equiv |T|$, $\mathcal{P} \equiv |P + (2/3)P^C_{\rm EW}|$, $\mathcal{T}' \equiv |T'|$, $\mathcal{P}' \equiv |P' + (2/3)P'^C_{\rm EW}|$. The ratio of $\Delta S = 1$ to $\Delta S = 0$ tree and penguin amplitudes are given by the corresponding ratios of CKM factors, $\mathcal{T}'/\mathcal{T} = |V_{us}/V_{ud}| \equiv r_u = 0.23$, $\mathcal{P}'/\mathcal{P} = |V_{ts}/V_{td}| \equiv r_t$. To introduce first-order SU(3)-breaking corrections, we note that in the $|T'|$ amplitude the W turns into an $\bar{s}$ quark instead of a d in $\mathcal{T}$. Assuming factorization for T, which is supported by experiments [23,24] and justified for $B \to \pi\pi$ and πK by the high momentum with which the two color-singlet mesons separate from one another, SU(3) breaking is given by the K/π ratio of decay constants

$$\frac{\mathcal{T}'}{\mathcal{T}} = \frac{|V_{us}|}{|V_{ud}|} \frac{f_K}{f_\pi} \equiv \tilde{r}_u. \tag{4}$$

Apart from small electroweak penguin terms, all amplitudes we consider are free of color-suppressed contributions, for which factorization might be more questionable. The situation would be very different were we to consider the amplitude for $B^0 \to \pi^0\pi^0$, where the color-suppressed contribution could be dominant.

In the penguin amplitudes (including electroweak penguin) of both $B^0 \to \pi^- K^+$ and $B^+ \to \pi^+ K^0$ the b quark turns into an $\bar{s}$ quark instead of a d in $B^0 \to \pi^+\pi^-$. Here we will denote the magnitude of the $\Delta S = 1$ penguin amplitude by $r_t\tilde{\mathcal{P}}$, to allow for SU(3) breaking. Since factorization is questionable for penguin amplitudes, one generally expects $\tilde{\mathcal{P}} \neq (f_K/f_\pi)\mathcal{P}$. We will assume that the phase δ_P is unaffected by SU(3) breaking. Since this phase is likely to be small [25], this assumption is not expected to introduce a significant uncertainty in the determination of the weak phases.

Assigning SU(3)-symmetric strong phases δ_T, δ_P to terms with specific weak phases, and taking account of SU(3) breaking, Eqs. (2) and (3) may be transcribed as

$$\begin{aligned} A_{\pi\pi} &= \mathcal{T} e^{i\delta_T} e^{i\gamma} + \mathcal{P} e^{i\delta_P} e^{-i\beta}, \\ A_{\pi K} &= \tilde{r}_u \mathcal{T} e^{i\delta_T} e^{i\gamma} - r_t \tilde{\mathcal{P}} e^{i\delta_P}, \\ A_+ &= r_t \tilde{\mathcal{P}} e^{i\delta_P}. \end{aligned} \tag{5}$$

It will be shown that the numerous *a priori* unknown parameters in Eq. (5), including the two weak phases $\alpha \equiv \pi - \beta - \gamma$ and γ, can be determined from the rate measurements of the above three processes and their charge conjugates.

The amplitudes for the corresponding charge-conjugate decay processes are simply obtained by changing the signs of the weak phases γ and β. We denote the charge-conjugate amplitudes corresponding to Eq. (5) by $A_{\pi\pi}$, $A_{\pi K}$, A_-, respectively. A state initially tagged as a B^0 or $\bar{B}^0$ will be

called $B^0(t)$ or $\overline{B^0}(t)$. The time-dependent decay rates of these states to $\pi^+\pi^-$ are given by

$$\Gamma(B^0(t)\to\pi^+\pi^-)=e^{-\Gamma t}\Big[|A_{\pi\pi}|^2\cos^2\Big(\frac{\Delta m}{2}t\Big)+|\overline{A}_{\pi\pi}|^2\sin^2\Big(\frac{\Delta m}{2}t\Big)+\mathrm{Im}(e^{2i\beta}A_{\pi\pi}\overline{A}^*_{\pi\pi})\sin(\Delta m t)\Big],$$

$$\Gamma(\overline{B^0}(t)\to\pi^+\pi^-)=e^{-\Gamma t}\Big[|A_{\pi\pi}|^2\sin^2\Big(\frac{\Delta m}{2}t\Big)+|\overline{A}_{\pi\pi}|^2\cos^2\Big(\frac{\Delta m}{2}t\Big)-\mathrm{Im}(e^{2i\beta}A_{\pi\pi}\overline{A}^*_{\pi\pi}\sin(\Delta m t)\Big]. \quad (6)$$

Measurement of these quantities determines $|A_{\pi\pi}|^2$, $|\overline{A}_{\pi\pi}|^2$, and $\mathrm{Im}(e^{2i\beta}A_{\pi\pi}\overline{A}^*_{\pi\pi})$. It is convenient to define sums and differences of the first two quantities, and we find

$$A\equiv\frac{1}{2}(|A_{\pi\pi}|^2+|\overline{A}_{\pi\pi}|^2)=\mathcal{T}^2+\mathcal{P}^2-2\mathcal{T}\mathcal{P}\cos\delta\cos\alpha,$$

$$B\equiv\frac{1}{2}(|A_{\pi\pi}|^2-|\overline{A}_{\pi\pi}|^2)=-2\mathcal{T}\mathcal{P}\sin\delta\sin\alpha,$$

$$C\equiv\mathrm{Im}(e^{2i\beta}A_{\pi\pi}\overline{A}^*_{\pi\pi})=-\mathcal{T}^2\sin 2\alpha+2\mathcal{T}\mathcal{P}\cos\delta\sin\alpha, \quad (7)$$

where we use $\beta+\gamma=\pi-\alpha$ and where we define $\delta\equiv\delta_T-\delta_P$.

The rates of the self-tagging modes π^-K^+, π^+K^- and π^+K^0 or $\pi^-\overline{K^0}$ determine $|A_{\pi K}|^2$, $|A_{\pi\overline{K}}|^2$ and $|A_+|^2$, respectively. Again, we take sums and differences of the first two, and find

$$D\equiv\frac{1}{2}(|A_{\pi K}|^2+|\overline{A}_{\pi K}|^2)=(\tilde{r}_u\mathcal{T})^2+\tilde{\mathcal{P}}'^2-2\tilde{r}_u\mathcal{T}\tilde{\mathcal{P}}'\cos\delta\cos\gamma,$$

$$E\equiv\frac{1}{2}(|A_{\pi K}|^2-|\overline{A}_{\pi K}|^2)=2\tilde{r}_u\mathcal{T}\tilde{\mathcal{P}}'\sin\delta\sin\gamma,$$

$$F\equiv|A_+|^2=|A_-|^2=\tilde{\mathcal{P}}'^2. \quad (8)$$

The rates for $B^+\to\pi^+K^0$ and $B^-\to\pi^-\overline{K^0}$ are expected to be equal, since only penguin amplitudes are expected to contribute to these processes. Here we have defined $\tilde{\mathcal{P}}'\equiv r_t\tilde{\mathcal{P}}$.

Measurement of the six quantities A–F suffices to determine all six parameters α, γ, $\mathcal{T}$, $\mathcal{P}$, $\tilde{\mathcal{P}}$, δ up to discrete ambiguities. The CKM parameter $r_t\equiv|V_{ts}/V_{td}|$, which is still largely unknown, is obtained from the unitarity triangle in terms of α and γ:

$$r_u r_t=\frac{\sin\alpha}{\sin\gamma}. \quad (9)$$

We note that

$$|A_{\pi K}|^2-|\overline{A}_{\pi K}|^2=-\Big(\frac{f_K}{f_\pi}\Big)\Big(\frac{\tilde{\mathcal{P}}}{\mathcal{P}}\Big)(|A_{\pi\pi}|^2-|\overline{A}_{\pi\pi}|^2), \quad (10)$$

which determines the magnitude of SU(3) breaking in the penguin amplitude, $\tilde{\mathcal{P}}/\mathcal{P}$. Relation (10) between the particle-antiparticle rate differences in $B\to\pi K$ and in $B\to\pi\pi$ was recently derived [26] in the SU(3) limit, $f_K/f_\pi\to 1$, $\tilde{\mathcal{P}}/\mathcal{P}\to 1$. The authors assumed for SU(3) breaking a value $\tilde{\mathcal{P}}/\mathcal{P}=f_K/f_\pi$ (based on factorization of penguin amplitudes) which in our approach is a free parameter to be determined by experiment. We expect it to differ from one by up to 30%.

Both sides of Eq. (10) are proportional to $\sin\delta$, and thus would vanish in the absence of a strong phase difference. In that case, one would have to assume a relation between $\tilde{\mathcal{P}}$ and $\mathcal{P}$ or some other constraint in order to obtain a solution. If, on the other hand, $\delta\neq 0$, leading to a rate asymmetry between the self-tagging decays $B^0\to\pi^-K^+$ and $\overline{B^0}\to\pi^+K^-$, the present method permits one to interpret that rate asymmetry in a manner independent of δ.

B. Likely ranges of observables

The amplitude for $B^0\to\pi^+\pi^-$ is expected to be dominated by the $\mathcal{T}$ contribution, while those for $B^0\to\pi^-K^+$ and $B^+\to\pi^+K^0$ are expected to be dominated by $\tilde{\mathcal{P}}'$. We shall choose units in which a branching ratio of 10^{-5} corresponds to a value of 1 for the rates A, D, and F. The normalizations of the other quantities are set accordingly. We shall also define the quantity

$$S\equiv A+D=\frac{1}{2}(|A_{\pi\pi}|^2+|\overline{A}_{\pi\pi}|^2+|A_{\pi K}|^2+|\overline{A}_{\pi K}|^2). \quad (11)$$

A combined sample of the decays $B^0\to\pi^+\pi^-$ and $B^0\to\pi^-K^+$ has been observed with a joint branching ratio of $(1.8^{+0.6+0.2}_{-0.5-0.3}\pm 0.2)\times 10^{-5}$ [27], so that $S=1.8\pm 0.65$. Equal mixtures of the two modes are most likely, corresponding to individual branching ratios of about 10^{-5} for $B^0\to\pi^+\pi^-$ and $B^0\to\pi^-K^+$. A similar branching ratio is expected for $B^+\to\pi^+K^0$ if the $\tilde{\mathcal{P}}'$ amplitude dominates $B\to\pi K$ decays, as seems likely. Thus, values of order 1 for A, D, and F are expected. We shall consider a range of values for these quantities, subject only to constraints on the lower and upper limits for S. As we shall see in Sec. III D, when δ can be neglected, this works out to a rule of thumb that $\mathcal{T}^2+\tilde{\mathcal{P}}'^2\approx 2$.

The detection of $B^+\to\pi^+K^0$ or $B^-\to\pi^-\overline{K^0}$ in practice will utilize the channels $B^\pm\to\pi^\pm K_S, K_S\to\pi^+\pi^-$, with a corresponding loss in efficiency of a factor of 3. We shall take this factor into account in estimating statistical errors on F.

The remaining quantities B, C, and E are harder to anticipate. The Schwarz inequality limits the value of $|C|$ to be less than or equal to A. In practice we find values of $|C|$ larger than 2 to be very unlikely. Thus, we shall consider values subject to this restriction. Both B and E will vanish if $\delta=0$. While a recent calculation [28] based on perturbative QCD [25] suggests that $\delta_T\approx 0$, $\delta_P\approx 9.5°$, $\delta\approx -9.5°$, the pos-

sibility of nonperturbative effects (such as strong final-state interactions differing in channels of different isospin) cannot be excluded. Thus, we shall consider the representative values $\delta=0$, 5.7°, 36.9°, 84.3°, 95.7°, 143.1°, 174.3°. We take only non-negative values since the error estimates are not affected by sign changes in δ. The nonzero values will be discussed in Sec. IV.

C. Constraints on the angles α and γ

Recent analyses of constraints on the CKM parameters include those in [29,30]. We shall visualize the allowed ranges of α and γ in order to choose illustrative sets of parameters.

We begin with the Wolfenstein parametrization [31] of CKM elements:

$$V_{cb}=A\lambda^2, \quad V_{ub}=A\lambda^3(\rho-i\eta), \quad V_{td}=A\lambda^3(1-\rho-i\eta), \tag{12}$$

as well as others not quoted explicitly, where $\lambda=0.22$. We shall assume [30] $V_{cb}=0.038\pm0.003$. (A slightly higher value is quoted in [32].) The measurement [30] $|V_{ub}/V_{cb}|=0.08\pm0.02$ based on charmless B decays implies $(\rho^2+\eta^2)^{1/2}=0.36\pm0.09$. The measurement of $B^0-\bar{B}^0$ mixing implies [32] $|V_{td}|=0.009\pm0.003$, which we shall interpret as implying $|1-\rho-i\eta|=1.0\pm0.3$. The requirement that the imaginary part of the K^0-$\bar{K}^0$ mixing amplitude due to CKM phases be responsible for the observed CP violation in the kaon system implies a hyperbola [30] $\eta(1-\rho+0.35)=0.48\pm0.20$, where the $1-\rho$ term in parentheses refers to the contribution of the top quark loop, while 0.35 refers to the charmed quark's contribution.

The allowed region in $(\rho,\ \eta)$ is shown in Fig. 1(a); the corresponding range of $(\alpha,\ \gamma)$ is depicted in Fig. 1(b) by a rather narrow band. The strong anticorrelation between α and γ is a function of the limited range of $\beta=\pi-\alpha-\gamma$, which is restricted to $6.6°\leqslant\beta\leqslant27°$ for the present set of parameters [30]. The band would not be quite so narrow using the parameters of one other analysis [29].

Three representative points, noted on the figure, are described in Table I. These correspond to extreme and central values of α and γ. A number of illustrative examples will be presented for these points.

Also shown on Fig. 1(b) is a linear least-squares fit to the points p_1, p_2, and p_3: $\gamma=175°-1.16\alpha$. Almost equally good is the approximate relation

$$\gamma=180°-1.2\alpha, \tag{13}$$

which we shall use in Sec. III A to simplify relations between $\pi\pi$ and πK rates.

D. Limitation associated with size of δ

Relation (10) can be written as

$$\frac{E}{B}=-\frac{f_K}{f_\pi}\frac{\tilde{\mathcal{P}}'}{\mathcal{P}'}. \tag{14}$$

We wish to evaluate the ratio $\tilde{\mathcal{P}}'/\mathcal{P}'$ to better than 30% [the anticipated magnitude of SU(3) breaking]. In this subsection we estimate the number of $\pi^+\pi^-$ events (and, correspondingly, the size of the other data samples) needed in order to measure B and E [see expressions (7) and (8)] to the required accuracy.

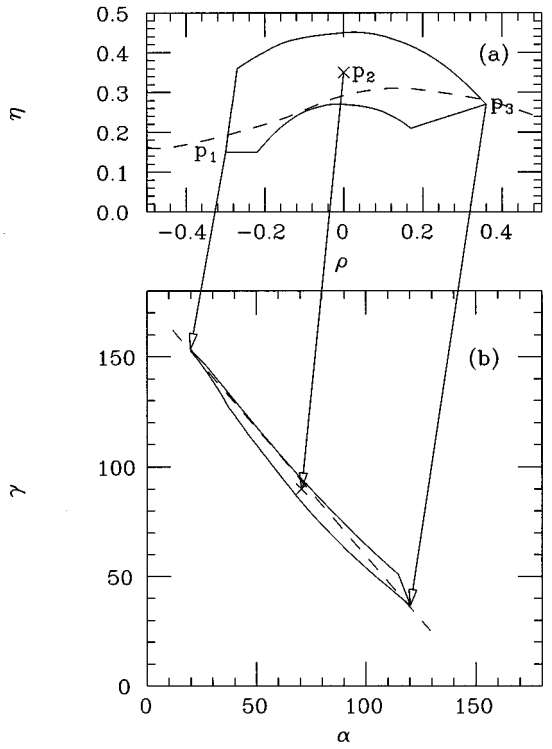

FIG. 1. Allowed ranges of CKM parameters (bounded by solid lines). The points p_1, p_2, and p_3 are described in Table I. (a) (ρ,η) plane; (b) as function of angles α and γ of the unitarity triangle. A linear least-squares fit to p_1, p_2, and p_3 yields $\gamma=175°-1.16\alpha$, as shown by the dashed straight line in (b); its map into the (ρ,η) plane is the dashed curve in (a).

Define the number of events averaged between particle and antiparticle decays:

$$\frac{N(B^0\to\pi^+\pi^-)+N(\bar{B}^0\to\pi^+\pi^-)}{2}\equiv N_{\pi\pi},$$

$$\frac{N(B^0\to\pi^-K^+)+N(\bar{B}^0\to\pi^+K^-)}{2}\equiv N_{\pi K}. \tag{15}$$

With equal branching ratios for $\pi^+\pi^-$ and $\pi^\mp K^\pm$, the present data sample would consist of about 10 events each for $N_{\pi\pi}$ and $N_{\pi K}$ [27]. The errors on A and B both scale as $N_{\pi\pi}^{1/2}$, while those on D and E scale as $N_{\pi K}^{1/2}$. Then in the samples of events used to measure A, B, D, and E, we expect

TABLE I. Representative points in the (ρ,η) plane and corresponding angles of the unitarity triangle.

Point	ρ	η	α (deg)	β (deg)	γ (deg)	r_t
p_1	−0.30	0.15	20.0	6.6	153.3	3.36
p_2	0	0.35	70.7	19.3	90.0	4.16
p_3	0.36	0.27	120.3	22.9	36.9	6.35

$$\delta N_A \simeq \delta N_B \simeq N_{\pi\pi}^{1/2}, \quad \delta N_D \simeq \delta N_E \simeq N_{\pi K}^{1/2}. \tag{16}$$

We take as illustrative parameters $\mathcal{T}=\widetilde{\mathcal{P}}'=\mathcal{P}'=1$, neglecting SU(3) breaking in the ratio $\widetilde{\mathcal{P}}'/\mathcal{P}'$. Recalling the expressions for B and E, we expect the numbers of events in the samples corresponding to these quantities to be

$$N_B = -2N_{\pi\pi} r_u \sin\delta \sin\gamma, \quad N_E = 2N_{\pi K}\widetilde{r}_u \sin\delta \sin\gamma, \tag{17}$$

where we have used Eq. (9). Consequently, the fractional errors on N_B and N_E are

$$\frac{|\delta N_B|}{|N_B|} \simeq \frac{1}{2N_{\pi\pi}^{1/2} r_u |\sin\delta \sin\gamma|}, \tag{18}$$

$$\frac{|\delta N_E|}{|N_E|} \simeq \frac{1}{2N_{\pi\pi}^{1/2} \widetilde{r}_u |\sin\delta \sin\gamma|}. \tag{19}$$

Thus the fractional error on the quotient N_B/N_E is the sum in quadrature of these two errors:

$$\frac{|\delta(N_B/N_E)|}{|(N_B/N_E)|} = \frac{1}{2N_{\pi\pi}^{1/2} r_u |\sin\delta \sin\gamma|} \left(1 + \frac{f_\pi^2}{f_K^2}\right)^{1/2}. \tag{20}$$

Demanding that this error be less than 30% as noted above and substituting the values of the constants, we find

$$N_{\pi\pi} \geqslant \frac{91}{\sin^2\delta \sin^2\gamma}. \tag{21}$$

This gives an idea of the data samples required to improve upon the assumption of no more than 30% SU(3) breaking in penguin amplitudes. More detailed estimates are postponed until Sec. IV. Meanwhile, we examine the special case in which the strong phase-shift difference δ vanishes.

III. VANISHING STRONG PHASE-SHIFT DIFFERENCE

Both the $\pi\pi$ parameter B and the πK rate asymmetry parameter E vanish when the strong phase-shift difference δ is zero. In that case, however, one can no longer use relation (10) to determine the ratio $\widetilde{\mathcal{P}}/\mathcal{P}$. One has four observables (A, C, D, and F) to determine five parameters (e.g., $\mathcal{T}$, $\mathcal{P}$, α, $\widetilde{\mathcal{P}}'$, and γ). One must make additional assumptions to obtain solutions. In this section we explore several such possibilities.

A. Simplified observables with $\delta=0$

When $\delta=0$, Eqs. (7) and (8) for A, C, and D become

$$A = \mathcal{T}^2 + \mathcal{P}^2 - 2\mathcal{T}\mathcal{P}\cos\alpha,$$

$$C = -\mathcal{T}^2 \sin(2\alpha) + 2\mathcal{T}\mathcal{P}\sin\alpha,$$

$$D = (\widetilde{r}_u\mathcal{T})^2 + \widetilde{\mathcal{P}}'^2 - 2\widetilde{r}_u\mathcal{T}\widetilde{\mathcal{P}}'\cos\gamma. \tag{22}$$

A simple relation follows from eliminating $\mathcal{P}$ between the first two of these equations:

$$(C/A)^2 = 4z(1-z),$$

where

$$z \equiv \mathcal{T}^2 \sin^2\alpha/A. \tag{23}$$

The Schwarz inequality bound $|C/A| \leqslant 1$ mentioned earlier is manifest here.

B. Linear relation between γ and α

A considerable simplification useful for anticipating the precision in determining α and γ is obtained by noting that α and γ are rather tightly correlated with one another [see Fig. 1(b)] as a result of the restricted range of β. As mentioned, the dependence can be approximated by a straight line. If we are concerned mainly with learning the sign of ρ and are not so concerned about the exact magnitude of $(\rho^2+\eta^2)^{1/2}$, we can substitute for γ in expression (22) for D, having already substituted $F=\mathcal{P}'^2$, and thus each measurement of D implies a relation between $\mathcal{T}$ and α.

An even greater simplification can be obtained if we neglect the term quadratic in $\mathcal{T}$ in D, and eliminate $\mathcal{T}$, $\mathcal{P}$, and $\widetilde{\mathcal{P}}'$ from the remaining equations involving A, C, D, and F. With the approximate formula (13) one has

$$\frac{\cos(1.2\alpha)}{\sin\alpha} = 2.6\,\frac{D-F}{\sqrt{F}}\,\frac{1}{\sqrt{A \pm \sqrt{A^2-C^2}}}. \tag{24}$$

The sign ambiguity stems from the fact that the equation for $\mathcal{T}\sin\alpha$ has two solutions. We can anticipate that the solution with $\mathcal{T}^2 \approx A$ is the most likely, as long as $\mathcal{P}$ is relatively small compared to $\mathcal{T}$, as generally anticipated. Since

$$(\mathcal{T}\sin\alpha)^2 = \frac{A \pm \sqrt{A^2-C^2}}{2}, \tag{25}$$

and since $|C|$ tends to be small when $\sin\alpha$ is near 1 (as for the point p_2), we anticipate that in that case we should choose the positive sign in the square root, and the argument of the overall square root in the denominator of the last fraction in Eq. (24) is about $2A$. On the other hand, when $|C|$ is fairly large (e.g., for points p_1 and p_3), the sign does not matter much, and the argument of the overall square root is about A.

For 100 $\pi^+\pi^-$ and 100 $\pi^\pm K^\mp$ events, the errors in A and D are about 10%. Assuming that the $|P'|$ contribution is dominant in D, the error on F will then be about 17% (because of the branching ratio of neutral kaons to $\pi^+\pi^-$). One then finds an error of about 0.55 in the right-hand side of Eq. (24) when α is near the middle of its range, and about 0.78 when α is near its lower or upper bounds. In Fig. 2(a) we plot the left-hand side of this equation, along with plotted points for $\alpha=20°$ (p_1), 71° (p_2), and 120° (p_3), with the errors in $\cos(1.2\alpha)/\sin\alpha$ of $\pm(0.78, 0.55, 0.78)$, respectively. The allowed region in (α,γ) is shown in Fig. 2(b) along with the line corresponding to $\gamma=180°-1.2\alpha$. The arrows designate values of α corresponding to p_1, p_2, and p_3.

When α is close to the center of its range, a sample of B decays corresponding to 100 events in each of the $\pi^+\pi^-$ and $\pi^\pm K^\mp$ channels allows one to narrow the allowed region of α by roughly a factor of 2. For the lowest or highest allowed values of α one does somewhat better. For more precise estimates, one would retain the $|T|^2$ term in D when $\alpha \simeq 90°$, and would be more precise about the error on C.

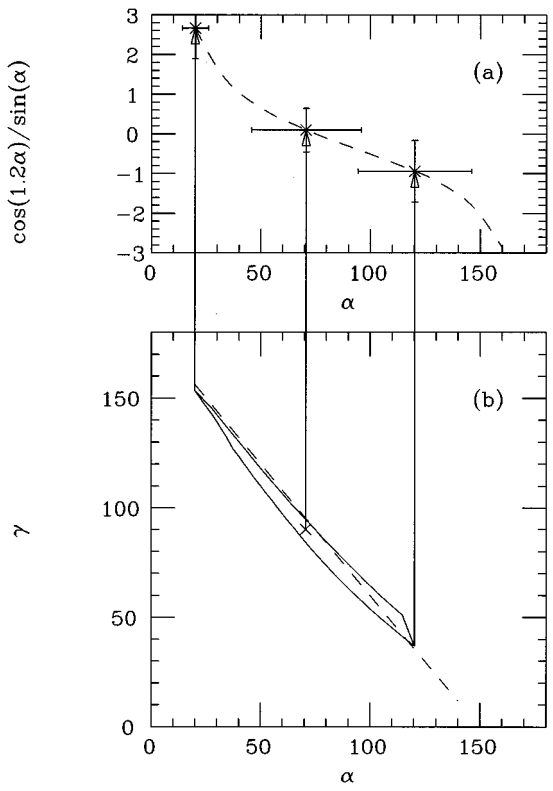

FIG. 2. (a) The function $\cos(1.2\alpha)/\sin\alpha$ as a function of α, and errors on α expected for a sample corresponding to 100 B^0 or $\overline{B^0}\to\pi^+\pi^-$ decays. The three points, from left to right, correspond to p_1, p_2, and p_3 of Table I, and $\delta=0$ is assumed. (b) Corresponding regions in the α-γ plane.

Let us for the moment neglect the small correction term in expression (7) for C. Then since $\sin 2\alpha$ can take on the same value for two values of α equally above and below $\pi/4$, there is a discrete ambiguity associated with negative values of C and values of $\alpha<\pi/2$. This ambiguity is likely to persist when we include the correction term. However, the addition of πK decay information appears capable of resolving this ambiguity, since it provides additional information on the angle γ which is highly correlated with α. For values of $\alpha>\pi/2$ and positive C only one solution (that for $\alpha<3\pi/4$) appears to be in the physical region, so we do not get the same sort of discrete ambiguity.

C. SU(3) assumption for penguin amplitudes

When $\delta=0$, as mentioned we are missing information on $\tilde{\mathcal{P}}'/\mathcal{P}'$. In the previous subsection we supplied this information by assuming a functional relation between α and γ. In the present subsection, we no longer assume such a relation, but simply assume this ratio to equal unity. (It was assumed to equal $f_K/f_\pi\approx 1.2$ in [10,26].) Under this assumption, we may drop the tilde symbols on $\tilde{\mathcal{P}}'$ in Eqs. (22). We may then plot contours of observables in the plane of $\mathcal{T}\equiv|T|$ vs $\mathcal{P}'\equiv|\mathcal{P}'|$ for various regions in the allowed parameter space.

Contours of fixed A are mainly sensitive to $\mathcal{T}$, while those of fixed D depend mainly on $\mathcal{P}'$. The slopes of the contours reflect the presence of constructive or destructive interference between $\mathcal{T}$ and $\mathcal{P}'$, depending on the signs of $\cos\alpha$ and $\cos\gamma$. Because of the strong anticorrelation between α and γ shown in Fig. 1, the contours of A and D are nearly perpendicular to one another for each of the three illustrated cases. This means that for each pair (α,γ), a measurement of A and D selects a point in the $(\mathcal{T},\mathcal{P}')$ plane with comparable errors on $\mathcal{T}$ and $\mathcal{P}'$ if the values and errors of A and D are comparable to one another.

A measurement of $F=|\mathcal{P}'|^2$ (the π^+K^0 or $\pi^-\overline{K^0}$ branching ratio, in units of 10^{-5}) must be consistent with the determination just made. Thus, a one-dimensional allowed set of points (α,γ) is chosen by the combined measurements of A, D, and F. The degree to which this choice is unique depends on being able to observe the effect of $\mathcal{T}-\mathcal{P}'$ interference in the measurement of D, since in the absence of the contribution from $\mathcal{T}$ one would have $D=F$. That is, the average $\pi^\pm K^\mp$ and π^+K^0 (or π^-K^0) rates would be the same in the absence of the $\mathcal{T}$ contribution to the $\pi^\pm K^\mp$ mode.

Once one has selected values of $\mathcal{T}$ and $\mathcal{P}'$ for a one-dimensional set of points in the (α,γ) plane, the value of C can be used to distinguish among those points. Positive values of C tend to be associated with negative values of $\sin(2\alpha)$ and hence with values of α greater than 90°. Such values correspond to (ρ,η) values lying inside a circle of radius 1/2 with center at $\rho=1/2$, $\eta=0$. These parameters correspond to roughly the right-hand one-third of the allowed regions in Figs. 1(a) and 1(b). The parameter spaces of Fig. 1 are much more sensitive to positive values of C than to negative values. We shall see such behavior again when we come to discuss a further simplification in the next subsection.

D. Information without π/K separation

The fact that the contours of A and D are nearly perpendicular to one another and have similar spacings in $\mathcal{T}$ and $\mathcal{P}'$, respectively, suggests that contours of

$$S=A+D=(1+\tilde{r}_u^{\,2})\mathcal{T}^2+(1+r_t^{-2})\mathcal{P}'^2-2\mathcal{T}\mathcal{P}'(r_t^{-1}\cos\alpha+\tilde{r}_u\cos\gamma) \tag{26}$$

may not depend very much on which set of allowed (α,γ) one chooses.

This expectation is borne out in Fig. 3. The observation that S is roughly independent of (α,γ) follows from the anticorrelation of $\cos\alpha$ and $\cos\gamma$. The sum of the average B^0 and $\overline{B^0}$ branching ratios to $\pi^+\pi^-$ and $\pi^\pm K^\mp$ leads to an approximate constraint on $\mathcal{T}^2+\mathcal{P}'^2$ roughly independent of CKM parameters within the allowed range. This is fortunate, since the CLEO Collaboration [27] measures precisely this sum, with only weak distinction at present between pions and kaons. (Improved particle identification at CLEO is foreseen in the future.) One may expect a similar measurement in some hadron collider experiments, such as the Collider Detector at Fermilab (CDF), unless specific steps are taken for particle identification.

A combined measurement of $\mathcal{T}^2+\mathcal{P}'^2$ and $F=\mathcal{P}'^2$ now can be used to determine each parameter. The determination of α and γ is now more simple-minded, albeit less precise, than in the previous section. Since our determination of $\mathcal{T}$ and $\mathcal{P}'$ is now independent of α and γ, we can use these parameters in Eq. (22) for C to plot contours of fixed C in the (α,γ) plane. (The variation with γ springs from the fact

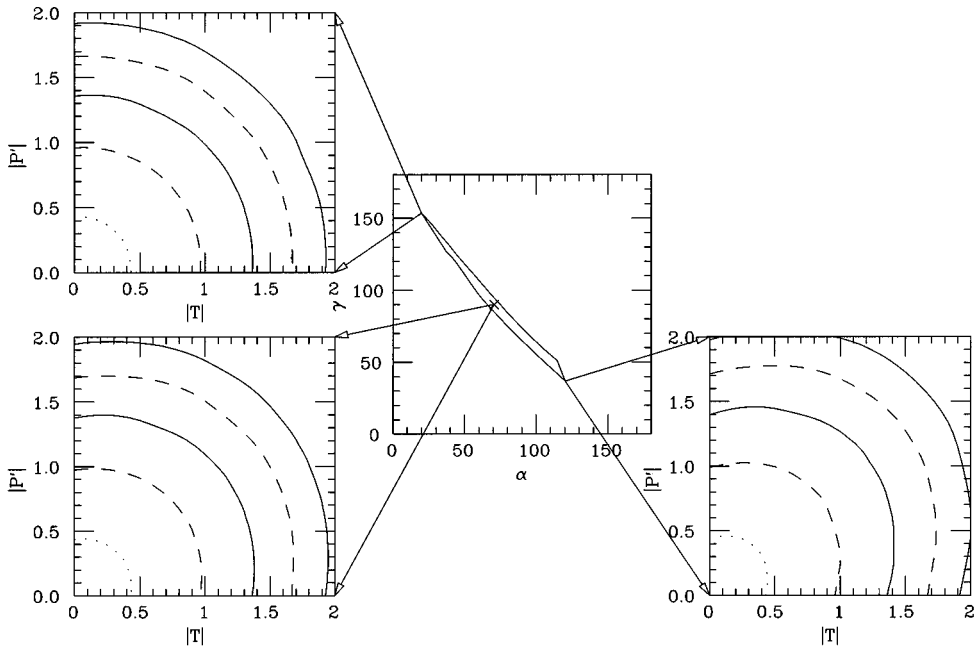

FIG. 3. Contours in the $|T|$-$|P'|$ plane of fixed $S=A+D$ (sum of average $\pi^+\pi^-$ and $\pi^\pm K^\mp$ branching ratio in units of 10^{-5}), for $\delta=0$. Dotted curves: $S=0.2$. Other curves, outward from origin: $S=1,2,3,4$.

that $r_u r_t=\sin\alpha/\sin\gamma$, as mentioned previously.) An example of such a contour is plotted in Fig. 4 for the representative values $\mathcal{T}=\mathcal{P}'=1.1$. One sees a fair amount of uncertainty for values of C near -0.7, where the contour intersects the allowed (α,γ) region in a wide range of points. This behavior is related to the discrete ambiguity noted at the end of Sec. III B. However, contours of positive C cut the allowed region at a larger angle and lead to a more highly constrained solution.

The measurement of C in the absence of particle identification is possible since one is following the time dependence of a decay rate in which one compares the decays of states which were initially B^0 and $\bar{B}^0$ to a combination of final states. The oscillations from which C is to be extracted are expected to stem only from the $\pi^+\pi^-$ final state.

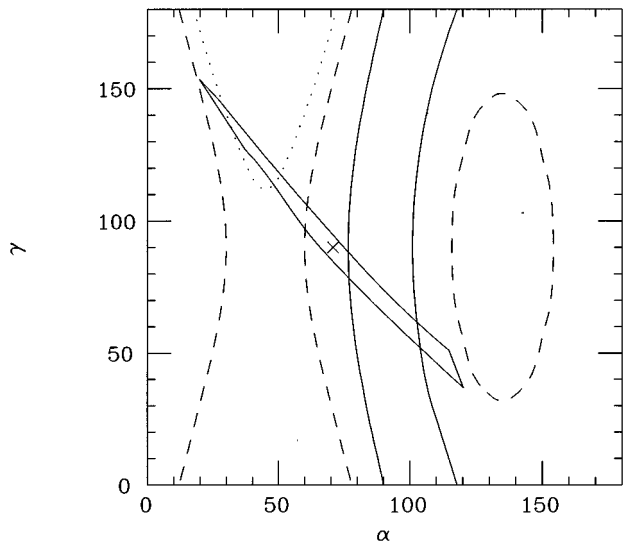

FIG. 4. Contours of fixed C for $|T|=|P'|=1.1$ as functions of α and γ, for $\delta=0$. Only those branches intersecting the allowed region are shown. Dotted curve: $C=-0.7$; dashed hyperbola: $C=-0.5$; solid curves, from left to right: $C=0$, 1; dashed ellipse: $C=1.5$.

The imposition of particle identification returns one to the situation of the previous section. As mentioned, to make efficient use of the information thus provided, one must be able to see the difference between D, where there is a small $\mathcal{T}$ contribution, and F, where there is none.

E. Results of a Monte Carlo simulation

We have explored numerically the case of $\delta=0$, $\tilde{\mathcal{P}}'=\mathcal{P}'$ using a Monte Carlo program which generates events with a statistical spread in the variables A, C, D, and F appropriate to data samples corresponding to a total of M decays of B^0 or $\bar{B}^0$ to $\pi^+\pi^-$. Scaling other quantities to the expected $\pi^+\pi^-$ rates, and recalling the discussion of Sec. II D, we then assume

$$\delta A=\delta C=\delta D=\delta F/\sqrt{3}=1/\sqrt{M}. \tag{27}$$

For $M=100$, 1000, 10 000 we then ask how well α and γ can be determined. Numerically this is accomplished by stepping α and γ through a range of values, accepting any solution which is within 2σ of the generated value for each parameter A,C,D,F, and averaging all such solutions. To allow for the possibility of multiple solutions, a cluster algorithm (described in the Appendix) is applied. We also restrict $10°\leqslant\alpha\leqslant130°$, $20°\leqslant\gamma\leqslant170°$, and $|\gamma-(175°-1.16\alpha)|\leqslant30°$ in accord with the allowed regions in Fig. 1. The results are shown in Fig. 5.

One sees a noticeable improvement with increased statistics. A clear distinction between the cases (p_1 or p_2) and p_3 is already possible with $M=100$. Satisfactory results for all three points are obtained for $M=1000$. The small ambiguity for p_1 appears to be related to the multiple intersections of the contours for negative C (Fig. 4) with the allowed region of parameter space. Errors are reduced further when M is increased to 10 000.

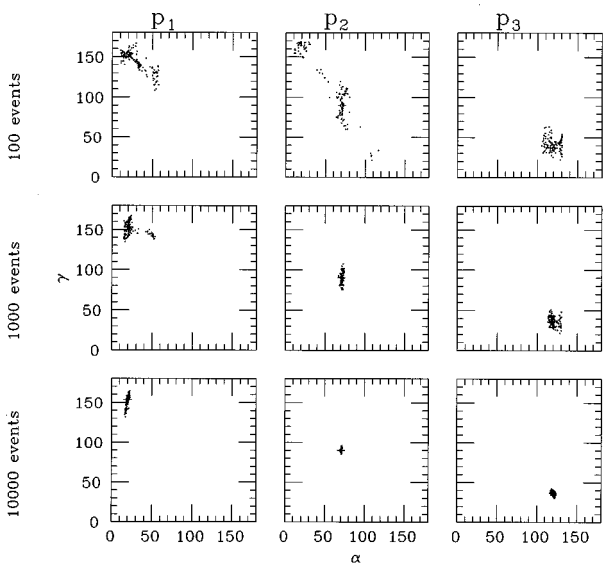

FIG. 5. Scatter plots in the α-γ plane of 100 events generated according to errors appropriate to samples of $M=100$, 1000, 10 000 events for the points p_1, p_2, p_3 of Table I, for $\delta=0$. Here the α and γ axes are plotted in degrees.

IV. ERROR ANALYSIS FOR GENERAL FINAL-STATE PHASES

In [14] we estimated the statistical accuracy of determining the weak phases α and γ using the present method to be at a level of 10%, given around 100 events in each channel. The theoretical uncertainty of the method is at a similar level, involving the following corrections all of which are of order a few percent: A correction from an electroweak penguin amplitude in $B^+\to\pi^+K^0$, corrections due to u and c quarks in the $B^0\to\pi^+\pi^-$ penguin amplitude, second-order SU(3) breaking in the magnitudes of weak amplitudes, first-order SU(3) breaking in the (small) strong phase of the penguin amplitude, and $O(f_B/m_B)$ annihilation amplitudes. In this subsection we analyze in more detail the precision on α and γ that can be attained with a given sample of events as a function of the parameters. We use a Monte Carlo program similar to that described in Sec. III E to generate events with a given Gaussian distribution in the parameters $A-F$ appropriate to a total sample corresponding to M $\pi^+\pi^-$ decays. We choose $\mathcal{T}=1$ and $\widetilde{\mathcal{P}}'=\mathcal{P}'=1$ for the purpose of generating events. In addition to the errors assumed in Eq. (27), we assume

$$\delta B=\delta E=1/\sqrt{M}. \tag{28}$$

The results are shown in Fig. 6.

The method clearly improves with increased statistics, in a manner roughly compatible with our estimate (21). Despite the presence of a large spread in values of α and γ, one can already distinguish the case p_3 from the cases p_1 and p_2 for $M=100$. The distinction between p_1 and p_2 appears to emerge by the time one reaches $M=1000$. On the other hand, one sees the distinct appearance of clusters of points, corresponding to the presence of discrete ambiguities. These ambiguities are to be distinguished from the one mentioned at the end of Sec. III B, and appear to be related to uncertainties in the value of the final-state phase. Their nature is best ascertained by referring to the case $M=10\,000$. One can detect up to three clusters of solutions. For example, in the case of input parameters in the vicinity of p_1, a final-state phase $\delta\approx 90°$ turns out to be ambiguous with two other cases, one with $\delta<90°$ and the other with $\delta>90°$, as one sees by referring to the corresponding plots of α vs δ shown in Fig. 7. For input parameters near p_2, the more serious ambiguities appear to occur for moderate or small values of δ. For input parameters near p_3, uncertainties present for $M=100$ and $M=1000$ appear to have largely disappeared by the time M reaches 10 000. This behavior may be related to the uniqueness of the solution provided by large positive C for points near p_3 in Fig. 4, but also points to the absence of ambiguities associated with the value of δ.

The discrete ambiguities mentioned previously are quite noticeable in Fig. 7; in addition, for δ near 180°, even the largest value of M does not lead to solutions in which that value is uniquely determined.

Note added. Numerical exact solutions have recently been generated for the cases considered here [33]. One chooses a set of input values of α, χ, and δ, along with a representative set of amplitudes $\mathcal{T}$, $\mathcal{P}$, $\mathcal{P}'$ as in the Monte Carlo estimates, and calculates the quantities $A-F$. Using these, one then solves back for α, γ, and δ. For some sets of the input values, as many as eight solutions were found. However, most of these can be excluded because the values of α and γ lie well outside of the region allowed in Fig. 1(b). All the correct solutions are obtained as expected, sometimes more than once. The remaining spurious ones, which show up as clusters in Figs. 6(c) and 7(c), are summarized in Table II. Many of these solutions involve the interchange $\gamma\leftrightarrow\delta$, which is a symmetry of the quantities D and E. Of course, α changes under this replacement.

V. CONCLUSIONS

To summarize, we have shown that measurements of the rates for B decays to modes involving charged pions and kaons in the final states can determine the shape of the unitary triangle, even in the absence of theoretical or experimental information about final-state phases. The full set of measurements involves the detection of the time-dependent rates for B^0 and $B^0\to\pi^+\pi^-$, and the rates for $B^0\to\pi^-K^+$, $\overline{B^0}\to\pi^+K^-$, and $B^\pm\to K_s\pi^\pm$. A rate asymmetry between $B^0\to\pi^-K^+$ and $B^0\to\pi^+K^-$ is needed in order to perform a solution for all necessary parameters. In the absence of this asymmetry, one can obtain partial information by noting the tight correlation between the angles α and γ of the unitarity triangle, or by assuming an SU(3) relation between strangeness-changing and strangeness-preserving penguin amplitudes. One can even dispense with particle identification, summing $\pi^+\pi^-$ and $\pi^\pm K^\mp$ modes, if only crude constraints on parameters are desired. As a result of the strong anticorrelation between α and γ in the physically allowed region of parameter space, the πK modes are particularly helpful in resolving a discrete ambiguity associated with the behavior of the function $\sin 2\alpha$ which would be present if one studied $\pi\pi$ modes alone.

In the simplest case examined, where the assumption of $\delta=0$ and the strong correlation between α and γ in the al-

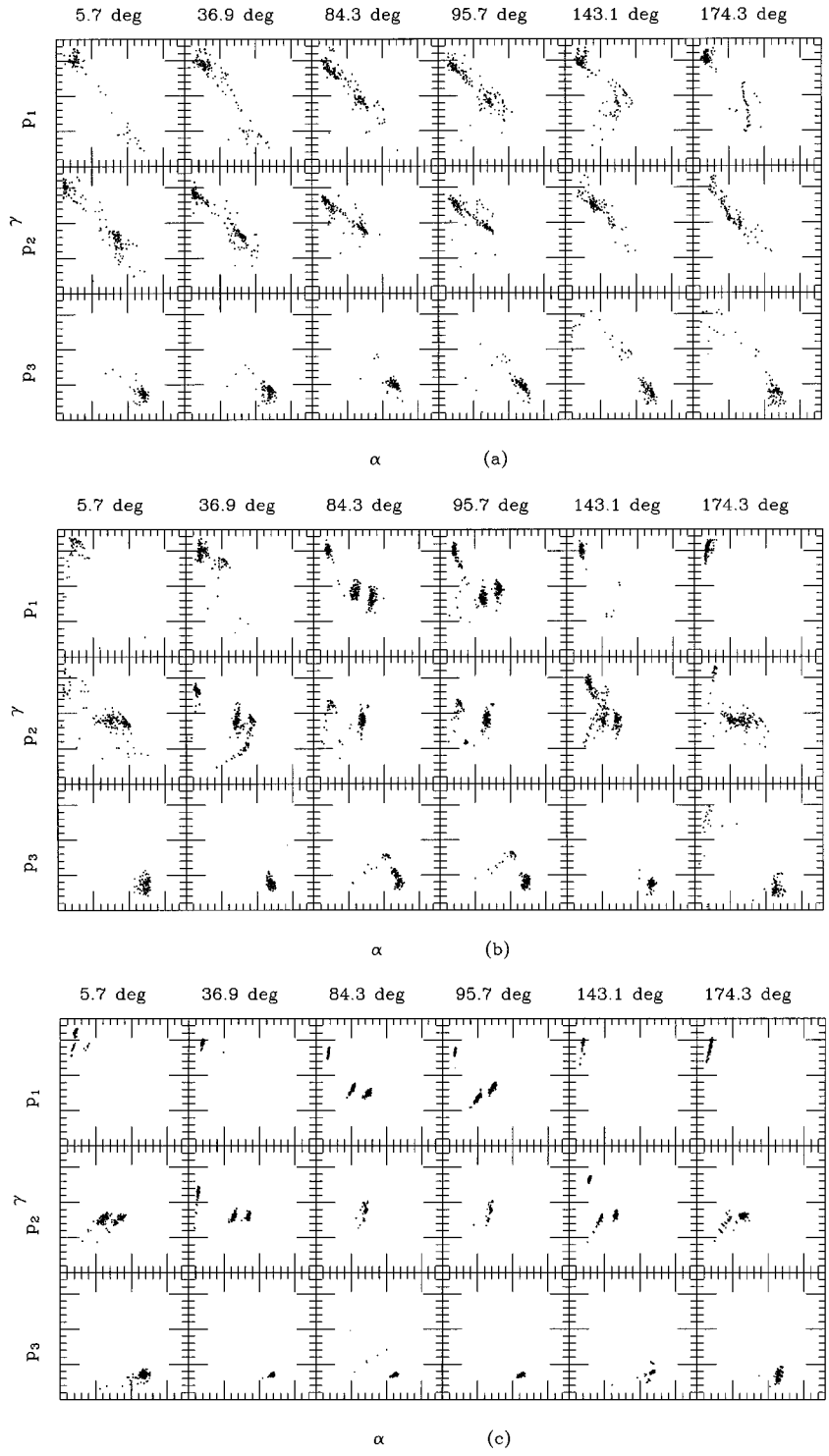

FIG. 6. Scatter plots in the α-γ plane for nonzero input values of δ (labels above columns) for the points p_1, p_2, p_3 of Table I (labels to left of rows). Here $0° \leqslant (\alpha,\gamma) \leqslant 180°$. (a) $M=100$; (b) $M=1000$; (c) $M=10\,000$.

lowed parameter space were utilized, we found that a sample of events corresponding to 100 $\pi^+\pi^-$ and 100 $\pi^\pm K^\mp$ events, with a correspondingly reduced number of detected $B^\pm \to K_S \pi^\pm$ decays, was sufficient to reduce the allowed region in parameter space by roughly a factor of two, depending on the values of the CKM angles.

In the more general case in which $\delta \approx 0$ but no relation between α and γ was assumed, we found that by assuming SU(3) symmetry for penguin amplitudes we could obtain unique solutions for α and γ, with some possibility of discrete ambiguity when α is small and γ is large (corresponding to $\rho<0$ in the language of the Wolfenstein parametrization). Even when a distinction between charged pions and charged kaons is not possible (Sec. III D), partial information on the parameters can be obtained, since the time-dependent effects are expected to be confined to the $\pi^+\pi^-$ channel and thus a measurement of the parameter C (defined in Sec. II) is still possible.

In the most general case of nonzero final-state phase differences δ we find that the program described here requires approximately $10^2/(\sin^2\delta \sin^2\gamma)$ decays of neutral B's to charged pions (and a similar number of πK events) in order

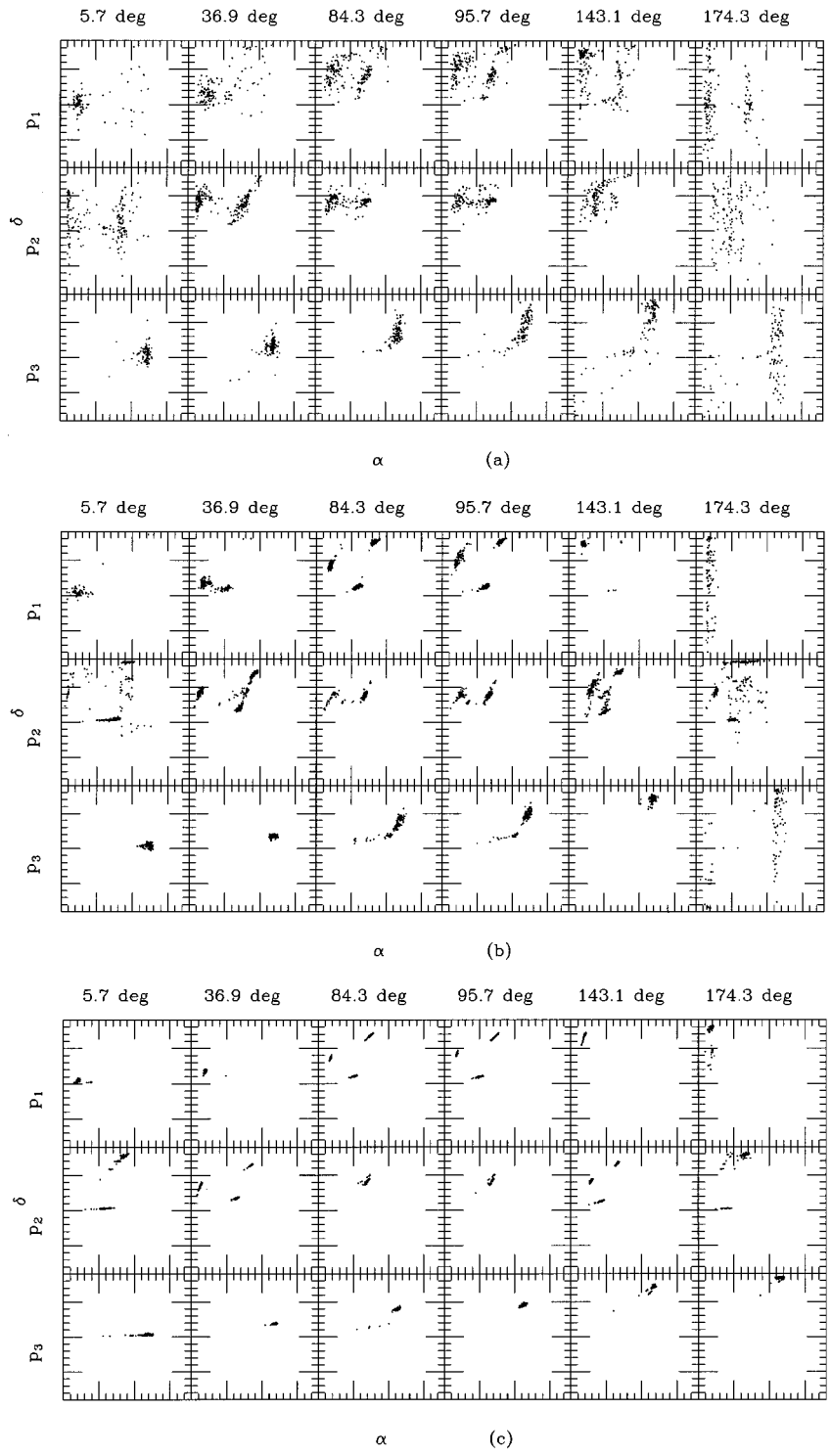

FIG. 7. Scatter plots in the α-δ plane for nonzero input values of δ (labels above columns) for the points p_1, p_2, p_3 of Table I (labels to left of rows). Here $0° \leqslant \alpha \leqslant 180°$; $-180° \leqslant \delta \leqslant 180°$. (a) $M=100$; (b) $M=1000$; (c) $M=10\,000$.

to free oneself from assumptions of SU(3) breaking at the 30% level in penguin amplitudes. A Monte Carlo program has shown that one begins to get useful information with 100 such decays (to be compared with about 10 in the present data sample). The full power of the method becomes apparent as the sample exceeds 1000 and approaches 10 000. Even under such circumstances, a discrete ambiguity remains associated with the size of final-state phases. Arguments external to those presented here [such as the allowed regions in the (α,γ) parameter space, the expected magnitude of SU(3) breaking, and the expected size of final-state phases] may be necessary to resolve such ambiguities.

ACKNOWLEDGMENTS

We thank J. Bjorken, F. De Jongh, H. Lipkin, D. London, H. Quinn, P. Sphicas, and S. Stone for fruitful discussions, and the CERN Theory Group for a congenial atmosphere in which part of this collaboration was carried out. A.D. wishes to thank G. Harris for valuable advice on Monte Carlo methods. M.G. and J.L.R. wish to acknowledge the respective hospitalities of the SLAC and Fermilab theory groups during

TABLE II. Output values of weak and strong phases, for given values of input weak and strong phases, in degrees. Only spurious solutions visible in the plots of Figs. 6(c) and 7(c) are shown.

$\alpha_{\rm in}$	$\gamma_{\rm in}$	$\delta_{\rm in}$	$\alpha_{\rm out}$	$\gamma_{\rm out}$	$\delta_{\rm out}$	Notes
20.0	153.4	84.3	59.3	93.1	23.6	
			82.8	83.4	152.3	a
		95.7	60.8	82.6	22.7	
			83.2	96.0	154.0	a,b
70.7	90.0	5.7	98.6	89.2	174.0	c
		36.9	15.2	127.2	82.8	
			92.5	88.8	140.6	c
		95.7	69.2	80.2	89.1	
			69.5	98.9	90.8	a
			65.8	88.0	74.2	
		143.1	31.1	145.4	91.1	a
			50.2	86.2	29.3	
120.3	36.9	5.7	135.7	34.0	6.5	
		143.1	121.7	42.6	148.4	

[a] $\gamma \leftrightarrow \delta$ interchange.
[b] β too small.
[c] $\alpha+\gamma>\pi$.

parts of this investigation, and J.L.R. thanks the Physics Department of the Technion for its hospitality. This work was supported in part by the United States—Israel Binational Science Foundation under Research Grant Agreement 94-00253/1, by the Fund for Promotion of Research at the Technion, and by the United States Department of Energy under Contract No. DE FG02 90ER40560.

APPENDIX: DETAILS OF CLUSTER ALGORITHM

Given a set of values for A, B, C, D, E, and F, the values of α, γ and δ are not necessarily determined uniquely. Apart from the ambiguities associated with the numerical nature of the algorithm, there can also be discrete ambiguities. In that case the set of triplets (α,γ,δ) consistent with all the observed quantities will form clusters in the (α,γ,δ) space, for any given set of A,B,C,D,E,F. The number of clusters corresponds to the number of discrete solutions and the spread within a cluster corresponds to the (numerical) error on that particular point. The average of all points in each cluster is taken to be the *central value* for that cluster and is plotted in Figs. 5, 6, and 7 as a single point. The number of points plotted for each data set is thus the number of discrete solutions for that data set.

The ambiguities associated with the numerical nature are expected to be *continuous*; i.e., for any point i to belong to a cluster, there should be at least one point j in the cluster such that $|\alpha_i-\alpha_j|\leq\Delta\alpha$, where $\Delta\alpha$ is the *least count* in α in the numerical algorithm. Two points i and j belonging to different clusters will fail to satisfy this condition. Different clusters can thus be separated from each other.

[1] For reviews see, for example, Y. Nir and H. R. Quinn, in *B Decays*, edited by S. Stone (World Scientific, Singapore, 1994), p. 362; I. Dunietz, *ibid*., p. 393; M. Gronau, in *Neutrino 94*, Proceedings of the XVI International Conference on Neutrino Physics and Astrophysics, Eilat, Israel, 1994, edited by A. Dar, G. Eilam, and M. Gronau [Nucl. Phys. B (Proc. Suppl.) **38**, 136 (1995)]; J. L. Rosner, lectures presented at VIII J. A. Swieca Summer School, Rio de Janeiro, 1995 (World Scientific, Singapore, in press) [Enrico Fermi Institute Report No. EF1 95-36, hep-ph/9506364].
[2] J. H. Christenson, J. W. Cronin, V. L. Fitch, and R. Turlay, Phys. Rev. Lett. **13**, 138 (1964).
[3] N. Cabibbo, Phys. Rev. Lett. **10**, 531 (1963); M. Kobayashi and T. Maskawa, Prog. Theor. Phys. **49**, 652 (1973).
[4] M. Gronau, Phys. Rev. Lett. **63**, 1451 (1989); D. London and R. D. Peccei, Phys. Lett. B **223**, 257 (1989); B. Grinstein, *ibid*. **229**, 280 (1989).
[5] R. Fleischer, Z. Phys. C **62**, 81 (1994); Phys. Lett. B **321**, 259 (1994); **332**, 419 (1994); N. G. Deshpande and X.-G. He, Phys. Rev. Lett. **74**, 26 (1995).
[6] M. Gronau and D. London, Phys. Rev. Lett. **65**, 3381 (1990).
[7] M. Gronau, O. F. Hernández, D. London, and J. L. Rosner, Phys. Rev. D **52**, 6374 (1995).
[8] M. Bauer, B. Stech, and M. Wirbel, Z. Phys. C **34**, 103 (1987); L. L. Chau *et al.*, Phys. Rev. D **43**, 2176 (1991); G. Kramer and W. F. Palmer, *ibid*. **52**, 6411 (1995).
[9] F. DeJongh and P. Sphicas, Phys. Rev. D **53**, 4930 (1996).
[10] J. Silva and L. Wolfenstein, Phys. Rev. D **49**, R1151 (1994).
[11] A. J. Buras and R. Fleischer, Phys. Lett. B **360**, 138 (1995).
[12] G. Kramer, W. F. Palmer, and Y. L. Wu, DESY Report No. DESY 95-246, hep-ph/9512341, 1995 (unpublished).
[13] R. Aleksan *et al.*, Phys. Lett. B **356**, 95 (1995).
[14] M. Gronau and J. L. Rosner, Phys. Rev. Lett. **76**, 1200 (1996).
[15] D. Zeppenfeld, Z. Phys. C **8**, 77 (1981).
[16] M. Savage and M. Wise, Phys. Rev. D **39**, 3346 (1989); **40**, 3127(E) (1989).
[17] L. L. Chau *et al.*, Phys. Rev. D **43**, 2176 (1991).
[18] M. Gronau, O. F. Hernández, D. London, and J. L. Rosner, Phys. Rev. D **50**, 4529 (1994).
[19] M. Gronau, O. F. Hernández, D. London, and J. L. Rosner, Phys. Rev. D **52**, 6356 (1995).
[20] M. Gronau and D. Wyler, Phys. Lett. B **265**, 172 (1991); M. Gronau, D. London, and J. L. Rosner, Phys. Rev. Lett. **73**, 21 (1994); M. Gronau *et al.*, Phys. Rev. D **52**, 6374 (1995); N. G. Deshpande and X.-G. He, Phys. Rev. Lett. **75**, 3064 (1995); M. Gronau and J. L. Rosner, Phys. Rev. D **53**, 2516 (1996).
[21] A. J. Buras and R. Fleischer, Phys. Lett. B **341**, 379 (1995).
[22] M. Gronau, Phys. Lett. B **300**, 163 (1993).
[23] T. Browder, K. Honscheid, and S. Playfer, in *B Decays*, edited by S. Stone (World Scientific, Singapore, 1994), p. 158.
[24] D. Bortoletto and S. Stone, Phys. Rev. Lett. **65**, 2951 (1990).
[25] M. Bander, D. Silverman, and A. Soni, Phys. Rev. Lett. **43**, 242 (1979); G. Eilam, M. Gronau, and J. L. Rosner, Phys. Rev. D **39**, 819 (1989); L. Wolfenstein, *ibid*., **43**, 151 (1991); J.-M. Gérard and W.-S. Hou, *ibid*., **43**, 2909 (1991); H. Simma, G. Eilam, and D. Wyler, Nucl. Phys. **B352**, 367 (1991).

[26] N. G. Deshpande and X.-G. He, Phys. Rev. Lett. **75**, 1703 (1995).
[27] CLEO Collaboration, D. M. Asner *et al.*, Phys. Rev. D **53**, 1039 (1996).
[28] G. Kramer and W. F. Palmer, Phys. Rev. D **52**, 6411 (1995).
[29] A. Ali and D. London, Z. Phys. C **65**, 431 (1995).
[30] Rosner [1].
[31] L. Wolfenstein, Phys. Rev. Lett. **51**, 1945 (1983).
[32] Particle Data Group, updated report on CKM elements by F. J. Gilman, K. Kleinknecht, and Z. Renk (unpublished).
[33] A. S. Dighe and J. L. Rosner, Phys. Rev. D (to be published).